Available online at www.sciencedirect.com
ScienceDirect
Journal of the European Ceramic Society 30 (2010) 3137–3143
www.elsevier.com/locate/jeurceramsoc

CeO_2–$YO_{1.5}$–$NdO_{1.5}$ system: An extensive phase relation study

V. Grover [a], S.V. Chavan [a], P. Sengupta [b], A.K. Tyagi [a,*]

[a] Chemistry Division, Bhabha Atomic Research Centre, Mumbai 400 085, India
[b] Materials Science Division, Bhabha Atomic Research Centre, Mumbai 400 085, India

Received 9 December 2009; received in revised form 4 June 2010; accepted 15 June 2010
Available online 24 July 2010

Abstract

The sub-solidus phase relations in the CeO_2–$YO_{1.5}$–$NdO_{1.5}$ system have been studied. About 45 compositions in the series $Ce_{1-x}(Y_{0.70}Nd_{0.30})_xO_{2-0.5x}$, $Y_{1-x}(Ce_{0.50}Nd_{0.50})_xO_{1.5+0.25x}$ and $Nd_{1-x}(Ce_{0.55}Y_{0.45})_xO_{1.5+0.275x}$ were prepared and characterized by powder XRD. In the $Ce_{1-x}(Y_{0.70}Nd_{0.30})_xO_{2-0.5x}$ series, there was a gradual transformation from the defective F-type cubic lattice to an ordered C-type phase with increasing x, whereas in the $Y_{1-x}(Ce_{0.50}Nd_{0.50})_xO_{1.5+0.25x}$ series, the C-type cubic lattice of yttria was retained over the entire range. In the $Nd_{1-x}(Ce_{0.55}Y_{0.45})_xO_{1.5+0.275x}$ system, the compositions with $NdO_{1.5}$ content greater than 95 mol% showed coexistence of hexagonal, monoclinic and cubic phases. A biphasic region of monoclinic and C-type cubic phases was observed as $NdO_{1.5}$ decreases from 90 to 70 mol%. All the compositions below 70 mol% $NdO_{1.5}$, were found to be C-type cubic solid solutions. The phase relations are distinctly characterized by an extensive range of cubic solid solutions, stable under the slow-cooled conditions. To the best of our knowledge, this is the first detailed sub-solidus study reported in CeO_2–$YO_{1.5}$–$NdO_{1.5}$ system.

Keywords: Powders-solid state reaction; X-ray methods; CeO_2

1. Introduction

Cerium oxide is a candidate material for variety of potential applications, e.g. optical glass-polishing, petroleum-cracking catalyst, gas sensors, etc.[1] Doped ceria is a potential solid electrolyte material for use in oxygen concentration cells, solid oxide fuel cells and in controlling air-to-fuel ratio in the automobile exhaust. In nuclear industry, CeO_2 is considered an important material as for its use as a surrogate for PuO_2.[2,3]

A number of reports have appeared in literature during the last few decades on alkaline-earth and rare-earth oxide doping in CeO_2, e.g. MgO,[4] CaO and SrO,[5] Sc_2O_3,[6] Y_2O_3, Gd_2O_3, La_2O_3, Nd_2O_3, Yb_2O_3,[7] La_2O_3 and Eu_2O_3.[8] In order to study new doped ceria materials (solid solutions and line compositions), several ceria based ternary phase relations have also been explored in detail. For example, ZrO_2–Y_2O_3–CeO_2,[9,10] Nd_2O_3–CeO_2–CuO, RuO_2–Y_2O_3–CeO_2,[11] Bi_2O_3–Y_2O_3–CeO_2,[12] ZrO_2–CeO_2–$LaO_{1.5}$.[13] Recently, various ternary relations have been reported on ceria based mixed oxides like CeO_2–ZrO_2–Gd_2O_3, CeO_2–ThO_2–ZrO_2 and CeO_2–Gd_2O_3–ThO_2 under the slow-cooled conditions.[14,15]

In the present study, a new ceria based ternary system, CeO_2–$YO_{1.5}$–$NdO_{1.5}$ has been investigated under the slow-cooled conditions. CeO_2 is known to have similar thermophysical properties as PuO_2. Hence, CeO_2 can act as a surrogate material for PuO_2 (fissile material) used in nuclear reactors, whereas $YO_{1.5}$ and $NdO_{1.5}$ are the fission products.[16] Thus, this ternary phase relation will be able to throw some light on kinds of phase fields present in the system containing these three components and will act as an invaluable database.

Detailed studies on the phase relations in the CeO_2–RE_2O_3 (RE = rare-earth) binary systems suggest that width of the two-phase region (i.e., coexistence of F and C-type phases) decreases with increasing RE^{3+} (rare-earth ion) radius.[17,18] Here again, it was difficult to distinguish the presence of a complete solid solution or a biphasic region ($Fluorite_{ss}$ and $C\text{-}type_{ss}$) by X-ray diffraction, as the cell constants tend to converge due to solid solution formation.[19–22] Pepin et al.[23] have determined the binary phase relations in CeO_2–RE_2O_3 system by quenching and have extrapolated it to ternary regions by taking CeO_2–Y_2O_3–Nd_2O_3 as the model reaction. It has been sug-

* Corresponding author. Tel.: +91 22 2559 5330; fax: +91 22 2550 5050/2551 9613.
E-mail addresses: aktyagi@barc.ernet.in, aktyagi64@rediffmail.com (A.K. Tyagi).

0955-2219/$ – see front matter © 2010 Elsevier Ltd. All rights reserved.
doi:10.1016/j.jeurceramsoc.2010.06.005

gested that the appearance of superlattice peaks (C-type phase) may be due to the presence of Ce_2O_3 obtained during quenching of the samples, and not due to an order–disorder phase transition as suggested in few other cases.[21,22]

For the present phase analysis, initially the corresponding binary phase relations in $YO_{1.5}$–$NdO_{1.5}$, CeO_2–$YO_{1.5}$ and CeO_2–$NdO_{1.5}$ systems were constructed. Suitable monophasic compositions were then chosen from each of these binary systems, and the ternary phase relations in CeO_2–$YO_{1.5}$–$NdO_{1.5}$ system have been worked upon. All the phase relation studies in this study have been performed under slow-cooled conditions.

2. Experimental procedure

Nd_2O_3 (AR grade), CeO_2 and Y_2O_3 (99.9%, obtained from Indian Rare-Earths) were used as the starting materials. Different nominal compositions were weighed, pelletized and then subjected to a heat treatment at 1200 °C for 36 h followed by another one at 1300 °C for 36 h, with intermittent grindings. After these heat treatments, each pellet was reground and mixed thoroughly, repelletized and finally annealed at 1400 °C for 48 h in static air followed by slow cooling to room temperature at the rate of 2 °C/min. XRD patterns were recorded on Philips X-ray diffractometer (Model PW 1710) with monochromatized Cu-Kα radiation. Silicon was used as an external standard. In order to determine the solubility limits, lattice parameters were refined by a least squares method.

A few representative compositions were also studied by EPMA (Electron Probe for Micro Analysis). Samples for EPMA studies were polished to 1 μm diamond finish by conventional metallographic techniques. The samples were coated with thin gold layer (≈10 nm) for ensuring conductivity. In order to acquire high contrast for back-scattered electron images, the acceleration voltage of 25–30 keV and the beam current around 1–4 nA were used.

3. Results and discussion

3.1. $Ce_{1-x}Y_xO_{2-x/2}$ and $Ce_{1-x}Nd_xO_{2-x/2}$

The detailed phase relations in CeO_2–$YO_{1.5}$ and CeO_2–$NdO_{1.5}$ systems have been studied and reported earlier by us.[24,25] The solubilities of about 45 mol% of Y^{3+} and 50 mol% of Nd^{3+} in CeO_2 lattice were observed in these studies. In case of $Ce_{1-x}Y_xO_{2-x/2}$, 45 mol% Y^{3+} could be dissolved in CeO_2 lattice retaining F-type (Fluorite) structure and beyond that a biphasic phase field consisting of F-type and C-type phases was observed. Similarly, in the case of $Ce_{1-x}Nd_xO_{2-x/2}$, 50 mol% Nd^{3+} could be dissolved in CeO_2 lattice retaining F-type structure, thereafter XRD studies showed the existence of C-type phase till 75 mol% Nd^{3+}. This is followed by a biphasic region of C-type phase and A-type phase (hexagonal). Interestingly, no biphasic region was observed between F- and C-type phases, though according to the phase rule, it should exist. We could not observe biphasic phase field by using lab source XRD. However, the presence of microdomains of C-type phase in F-type lattice cannot be absolutely ruled out, based on powder XRD data alone, due to the close similarity between F-type and C-type structures. Similar situation was observed in case of CeO_2–Gd_2O_3 system.[26] Later on, we reported detailed Raman spectroscopic studies on CeO_2–Gd_2O_3 system which indicated at the presence of C-type microdomains in F-type lattice and vice versa.[27] It may be added that the Electron Diffraction can unequivocally confirm the presence or absence of any narrow biphasic (F + C) region in this series. These studies are underway and would be reported subsequently.

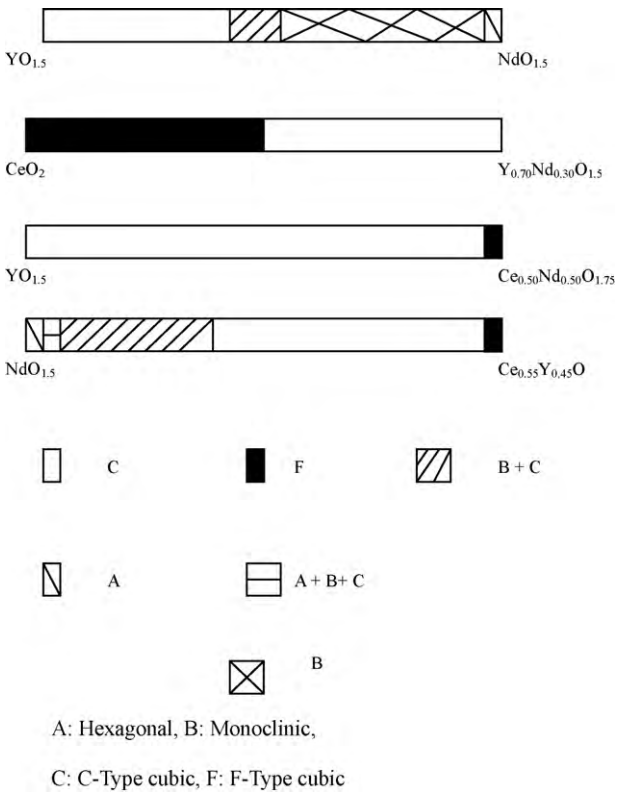

Fig. 1. Bar diagram representing phase relations in (a) $Y_{1-x}Nd_xO_{1.5}$; (b) $Ce_{1-x}(Y_{0.70}Nd_{0.30})_xO_{2-0.5x}$ series; (c) $Y_{1-x}(Ce_{0.50}Nd_{0.50})_xO_{1.5+0.25x}$ series; (d) $Nd_{1-x}(Ce_{0.55}Y_{0.45})_xO_{1.5+0.275x}$ series.

3.2. $Y_{1-x}Nd_xO_{1.5}$ series

The phase relations in this system are given by the bar diagram in Fig. 1(a). The end member Y_2O_3 has a C-type cubic structure and the other end member Nd_2O_3 has a hexagonal structure. It was observed that the C-type cubic structure of $YO_{1.5}$ was retained till 30 mol% Nd^{3+} substitution, i.e., till the nominal composition $Y_{0.70}Nd_{0.30}O_{1.50}$. The lattice parameter of the C-type solid solution increases with increase in mol% Nd^{3+} as is shown in Fig. 2(a). Beyond the nominal composition $Y_{0.70}Nd_{0.30}O_{1.50}$, peaks due to monoclinic phase of $NdO_{1.5}$ start appearing. Subsequently, there was a phase separation into C-type solid solution ($NdO_{1.5}$ in $YO_{1.5}$ lattice) and a monoclinic solid solution ($YO_{1.5}$ in $NdO_{1.5}$ lattice). This biphasic region exists till the composition $Y_{0.50}Nd_{0.50}O_{1.50}$. Beyond this composition, the C-type peaks disappear and only the mon-

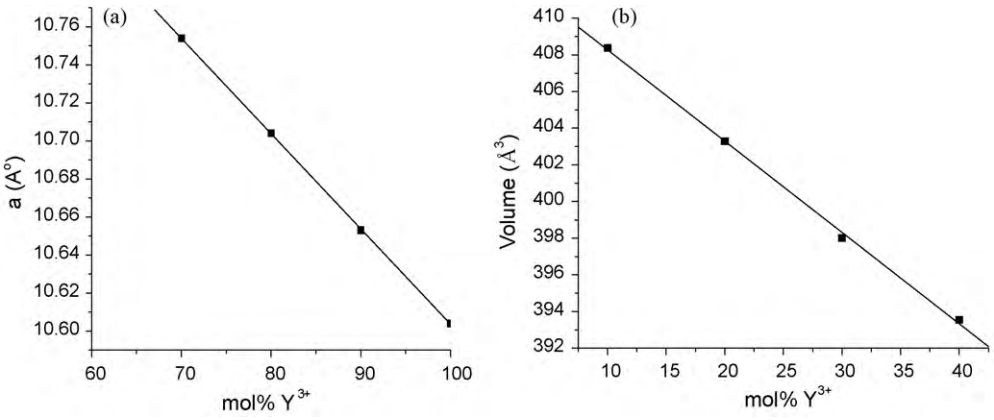

Fig. 2. Variation of lattice parameter with mol% Y^{3+} in $Y_{1-x}Nd_xO_{1.5}$: (a) variation of '*a*' of C-type phase and (b) variation of volume of monoclinic phase.

oclinic phase could be observed. The monoclinic phase thus extends from the composition $Y_{0.40}Nd_{0.60}O_{1.50}$ to the composition $Y_{0.10}Nd_{0.90}O_{1.50}$.

Few typical XRD patterns representing different phase fields obtained in this system are given in Fig. 3. It was observed that on incorporating 10 mol% $YO_{1.5}$ into $NdO_{1.5}$, the monoclinic phase (B-type) of $NdO_{1.5}$ is obtained. As explained by Adachi and Imanaka[28] that rare-earth oxides exist as three different polymorphs, designated as A (hexagonal), B (monoclinic) and C (cubic) for RE_2O_3 (RE = rare-earths) at temperatures below 2000 °C, depending upon the rare-earth ionic sizes. In general, on going from La^{3+} to Lu^{3+}, the structure of RE_2O_3 changes from A-type to B-type to C-type, as the ionic size of the rare-earth ion decreases. It may be noted that in the present system, Nd_2O_3 is hexagonal at room temperature, i.e., A-type. Also, according to the phase diagram constructed by Adachi and Imanaka,[28] the A-phase of $NdO_{1.5}$ cannot be converted to B or C-phase by means of temperature alone. A striking observation of this investigation is the stabilization of B-type monoclinic phase of Nd_2O_3 on substitution of about 10 mol% Y^{3+} which is otherwise difficult to obtain even at higher temperatures. The nominal composition $Nd_{0.90}Y_{0.10}O_{1.5}$ was characterized by the Rietveld refinement of the observed powder XRD data. The typical refined unit cell parameters for this nominal composition are: 14.2761(3), 3.6449(1), 8.9022(2) Å and $\beta = 100.391(2)^\circ$, $V = 455.62(2)$ Å^3. The Rietveld refinement results confirm the monoclinic rare-earth oxide structure with Nd^{3+} occupying a seven-coordinated (capped distorted trigonal prism type) polyhedra and six-coordinated (trigonal prism) polyhedra. The crystal structure is built from the edge sharing of these polyhedra. A noteworthy observation that emerges out of the refinement studies is that the Y^{3+} prefers six-coordinated polyhedral sites instead of being randomly distributed over all the Nd^{3+} sites, which is accounted by the smaller ionic radius of Y^{3+} as compared to the Nd^{3+}.

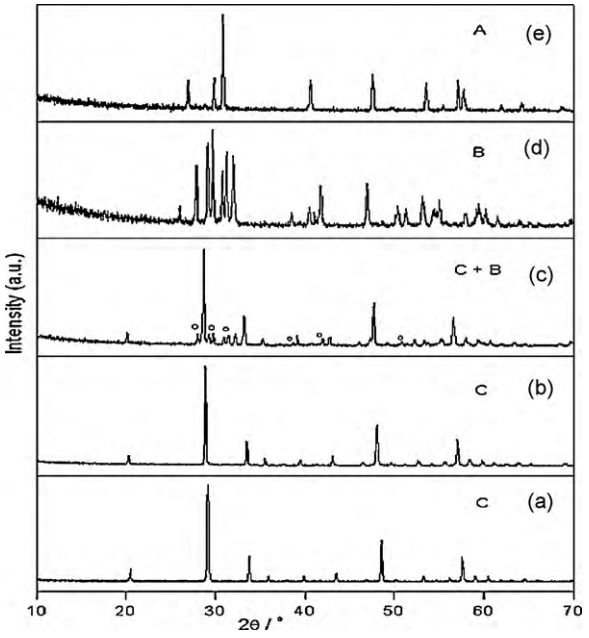

Fig. 3. XRD patterns in $Y_{1-x}Nd_xO_{1.5}$ system: (a) Y_2O_3; (b) $Y_{0.80}Nd_{0.20}O_{1.50}$; (c) $Y_{0.60}Nd_{0.40}O_{1.50}$; (d) $Y_{0.30}Nd_{0.70}O_{1.5}$; (e) Nd_2O_3.

It may be noted that a similar stabilization of C-type phase of $NdO_{1.5}$ was observed on incorporating of about 32.5 mol% CeO_2 into the $NdO_{1.5}$ lattice.[25] There, in the case of Ce^{4+} doped $NdO_{1.5}$, the average cationic size in $Ce_{1-x}Nd_xO_{2-x/2}$ appears to further decrease to an extent as to fall in the C-type stability region. In the present case, apparently the decrease in the average cationic size, on Y^{3+} substitution, is just sufficient to stabilize the B-type phase and not enough to get the C-type phase of $NdO_{1.5}$ (ionic size of $Ce^{4+} = 0.90$ Å and $Y^{3+} = 0.93$ Å in cubic coordination).

As mentioned earlier, the monoclinic phase prevails from the composition $Y_{0.10}Nd_{0.90}O_{1.5}$ to the composition $Y_{0.40}Nd_{0.60}O_{1.50}$. The monoclinic lattice parameters show a decreasing trend with increase in mol% Y^{3+}. The variation in the volume of the monoclinic phase as a function of composition is shown in Fig. 2(b). This trend can be explained by the ionic size of Y^{3+} being smaller than that of Nd^{3+} (for $Y^{3+} = 0.93$ Å and for $Nd^{3+} = 1.01$ Å in eight-fold coordination). Thus, it can be summarized that the system $Y_{1-x}Nd_xO_{1.5}$ consists of three phase fields, i.e., (i) single-phasic C-type cubic solid solution of $NdO_{1.5}$ into $YO_{1.5}$ (ii) a biphasic region of C-type cubic $YO_{1.5}$ and monoclinic phase of $YO_{1.5}$ into $NdO_{1.5}$ and (iii) a single-phasic monoclinic solid solution of $YO_{1.5}$ into $NdO_{1.5}$.

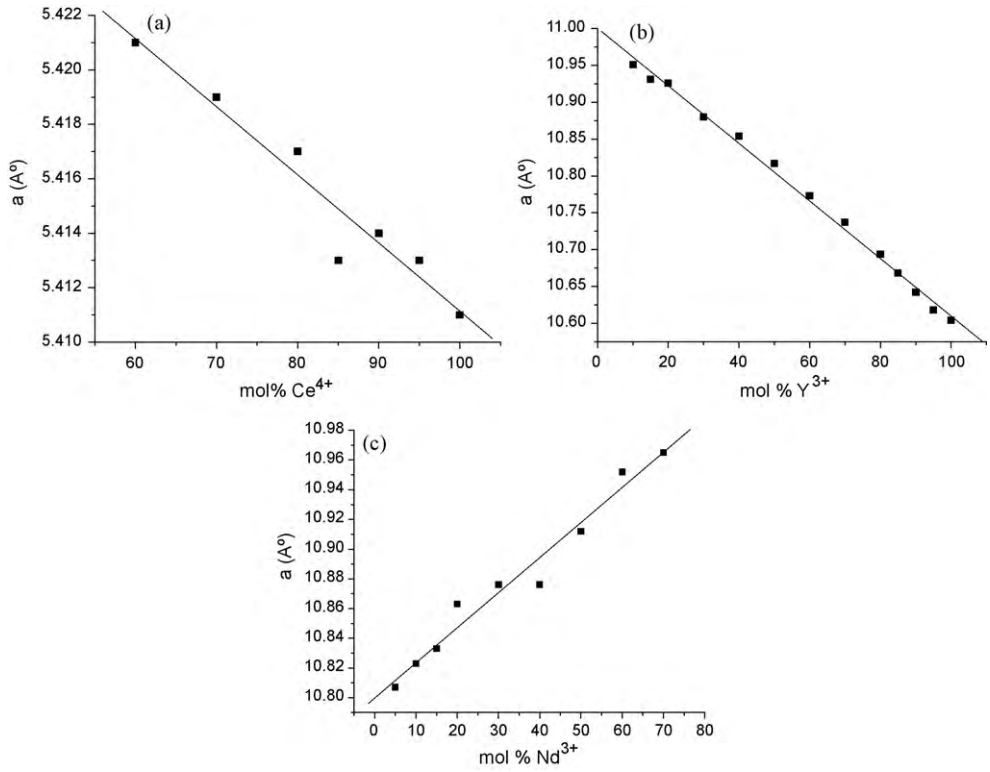

Fig. 4. Variation of lattice parameter of (a) F-type solid solution with mol% Ce^{4+} in $Ce_{1-x}(Y_{0.70}Nd_{0.30})_xO_{2-0.5x}$ series; (b) C-type solid solution with mol% Y^{3+} in $Y_{1-x}(Ce_{0.50}Nd_{0.50})_xO_{1.5+0.25x}$ series; (c) C-type solid solution with mol% Nd^{3+} in $Nd_{1-x}(Ce_{0.55}Y_{0.45})_xO_{1.5+0.275x}$ series.

The end member $NdO_{1.5}$ exists in hexagonal phase, which was not observed in any other composition of this system.

Based on the phase relation studies in the binary mixed oxide systems viz. CeO_2–$YO_{1.5}$, CeO_2–$NdO_{1.5}$, $YO_{1.5}$–$NdO_{1.5}$, the monophasic compositions corresponding to the upper solubility limit of the guest species were identified. These compositions were $Ce_{0.55}Y_{0.45}O_{1.775}$, $Ce_{0.50}Nd_{0.50}O_{1.75}$, and $Y_{0.70}Nd_{0.30}O_{1.5}$ for the corresponding binary systems. A detailed phase relation analysis was then carried out between these compositions the end members viz., CeO_2, $YO_{1.5}$ and $NdO_{1.5}$.

3.3. $Ce_{1-x}(Y_{0.70}Nd_{0.30})_xO_{2-0.5x}$ series

From the phase relation studies between $YO_{1.5}$ and $NdO_{1.5}$ mentioned earlier, the composition $Y_{0.70}Nd_{0.30}O_{1.5}$ (upper solubility limit with C-type lattice) was fixed as one of the end member and CeO_2 was taken as the other end member. The phase relation in this system is depicted by the bar diagram in Fig. 1(b). It is observed that the F-type cubic lattice of CeO_2 was retained till $x = 0.50$, i.e., till the composition $Ce_{0.50}(Y_{0.35}Nd_{0.15})O_{1.75}$. Thus it can be inferred that both 35 mol% of $YO_{1.5}$ and 15 mol% of $NdO_{1.5}$ could be simultaneously dissolved in the CeO_2 lattice. The lattice parameter values were found to increase, as the concentration of the trivalent ions (Y^{3+}, Nd^{3+}) increases as shown in Fig. 4(a). Earlier studies carried out by us in the Ce–Y–O system showed different results.[24] In that case, with the substitution of Ce^{4+} by Y^{3+}, a decreasing trend in lattice parameter was observed, despite slightly larger size of Y^{3+} (the ionic radii of Ce^{4+} and Y^{3+} are 0.90 and 0.93 Å, respectively in the eight-fold coordination[1]). The aliovalent substitution of a tetravalent ion by a trivalent ion is accompanied by simultaneous incorporation of oxygen ion vacancies. Thus in Ce–Y–O system, the observed variation in the lattice parameter trend was the compromise obtained between increase in lattice parameter due to increase in average ionic radii and decrease due to the incorporation of oxygen vacancies with the latter controlling the observed trend. However, similar studies carried on the Ce–Nd–O system showed that the substitution by a considerably larger ion like Nd^{3+} results in an increase in the cell parameter.[25] It is evident that in the case of Ce–Nd–O system the relative ionic size effect dominates over the oxygen vacancy effect. In the present case, the trend is a combination of the abovementioned cases. Hence, herein the increase in the lattice parameter is not as steep and remains somewhat close to that of pure CeO_2. Thus, clearly the incorporation of vacancies causes a reduction in the cell dimensions, while the substitution of the trivalent cations cause lattice expansion. However, as the concentration of $NdO_{1.5}$ is not too high (15 mol%) compared to $YO_{1.5}$, the net increase in the lattice parameter value is only marginal. At and beyond the composition $Ce_{0.40}(Y_{0.42}Nd_{0.18})O_{1.70}$, a C-type ordered phase was observed, which extends up to the other end of the CeO_2 deficient region. Thus, as the concentrations of Y^{3+} and Nd^{3+} in CeO_2 increase, more and more oxygen ion vacancies are created, which are the driving force for ordering, and hence result into a C-type ordered lattice. It was observed that the lattice param-

[1] VCH Periodic Table of Elements, 1995, Compiled by Fluck & Heumann.

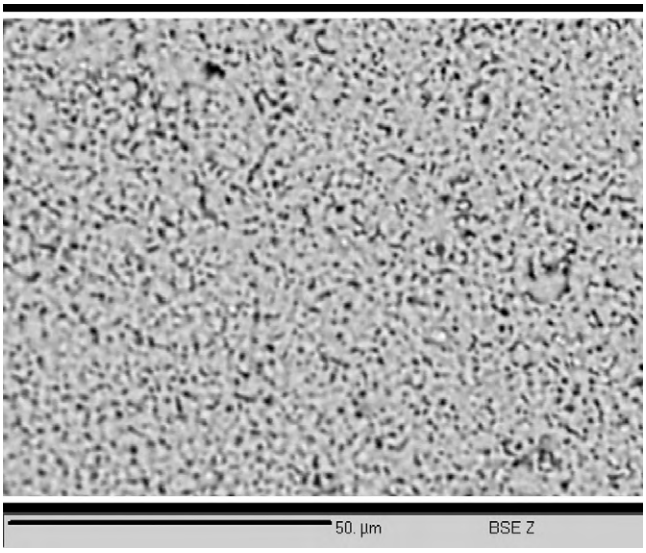

Fig. 5. Back-scattered image for the nominal composition $Ce_{0.15}Y_{0.595}Nd_{0.255}O_{1.575}$. The dark pots correspond to the pores as confirmed by EDX analysis.

eter of C-type phase decreases (though not substantially) with increasing dopant concentration. Again this could be because the lattice contraction caused by the large concentration of vacancies appears to predominate over the lattice expansion caused by the increase in average cationic size. An important observation in this case is a complete miscibility of $(Y_{0.70}Nd_{0.30})O_{1.50}$ and CeO_2 throughout the range of compositions.

It was observed that in the binary system CeO_2–$YO_{1.5}$, the solubility limit of Y^{3+} in CeO_2 was about 45 mol%[24] and that in the system CeO_2–$NdO_{1.5}$, the solubility of Nd^{3+} in CeO_2 was about 67.5 mol%.[25] In the present case, however, much higher net trivalent ion concentration could be accommodated in the CeO_2 lattice without any phase separation. This observation can be attributed to an optimum ionic size difference between the Ce^{4+} and weighted average size of Y^{3+} and Nd^{3+}.

EPMA (Electron Probe for micro analysis) studies were also done on some of the representative samples. Fig. 5 gives a typical back-scattered image for the nominal composition $Ce_{0.15}Y_{0.595}Nd_{0.255}O_{1.575}$ which shows this composition to be single-phasic. The dark colored features observed in the SEM image are the pores as is shown by EDX analysis. Also, the composition given by EDX analysis is in good agreement with the nominal composition.

3.4. $Y_{1-x}(Ce_{0.50}Nd_{0.50})_xO_{1.5+0.25x}$ series

In this series, the end members viz. $YO_{1.5}$ and $Ce_{0.50}Nd_{0.50}O_{1.75}$ belong to the C-type and F-type cubic symmetry, respectively. The bar diagram given in Fig. 1(c) depicts the phase relation obtained in this system. Interestingly, unlike the previous series, the entire range of compositions are single-phasic showing a C-type ordering throughout, i.e., a C-type phase field is obtained from $Y_{0.95}Ce_{0.025}Nd_{0.025}O_{1.512}$ to $Y_{0.10}Ce_{0.45}Nd_{0.45}O_{1.725}$. For the composition, $Y_{0.05}(Ce_{0.475}Nd_{0.475})O_{1.737}$, there was a complete transformation from C-type lattice to a F-type defect fluorite phase. When $Ce_{0.50}Nd_{0.50}O_{1.75}$ is incorporated into $YO_{1.5}$ lattice, the substitution of Nd^{3+} in place of Y^{3+} would retain the effective concentration of oxygen vacancies, and therefore the extent of ordering. However, the substitution of Ce^{4+} in place of Y^{3+} causes a net filling of those oxygen vacancies, which gradually diminish the ordering of vacancies. It may be noted that the ordered C-type phase in $REO_{1.5}$ is observed due to the ordering of 0.5 oxygen vacancies. This filling of vacancies with increase in amount of $Ce_{0.50}Nd_{0.50}O_{1.75}$ leads to the transformation of an ordered C-type phase to a disordered F-type phase since the driving force for ordering, i.e., vacancies, decreases gradually on increasing the 'x' value. Therefore, with increase in concentration of Ce^{4+} there is a tendency for randomization of the oxygen ion vacancies resulting in reduced intensity of the superlattice peaks and eventually in the nominal composition $Y_{0.05}(Ce_{0.475}Nd_{0.475})O_{1.737}$, the ordering is completely lost resulting in a F-type phase. There is a gradual increase in lattice parameter values from 10.604 Å for pure $YO_{1.5}$ to 10.971 Å for the composition $Y_{0.05}(Ce_{0.475}Nd_{0.475})O_{1.737}$ as shown in Fig. 4(b). The size of Nd^{3+} (1.01 Å) is much larger than Y^{3+} (0.93 Å), resulting in the expansion of the lattice.

3.5. $Nd_{1-x}(Ce_{0.55}Y_{0.45})_xO_{1.5+0.275x}$ series

The end members in this series viz. $NdO_{1.5}$ and $Ce_{0.55}Y_{0.45}O_{1.775}$ belong to the hexagonal (A-type) and F-type cubic symmetry, respectively. The phase relation in this system is represented by the bar diagram shown in Fig. 1(d). A few typical XRD patterns describing the various phase fields obtained in this system are given in Fig. 6. Unlike the earlier two cases, where there was a complete solid solution formation throughout the homogeneity range, various mixed phases seem to appear in this case. For example, the composition $Nd_{0.95}(Ce_{0.028}Y_{0.022})O_{1.513}$ showed the coexistence of three phases viz. A (hexagonal), B (monoclinic) and C (C-type cubic). The hexagonal phase, that of $NdO_{1.5}$, was the majority phase showing no change in the lattice parameter value suggesting that no Ce^{4+} or Y^{3+} could be incorporated in the hexagonal lattice of $NdO_{1.5}$. For the next composition $Nd_{0.90}(Ce_{0.055}Y_{0.045})O_{1.527}$, there was a complete transformation of the hexagonal phase to the monoclinic phase due to the presence of $YO_{1.5}$. Similar results were observed in the case of phase relation studies in Nd–Y–O system. At and beyond the composition $Nd_{0.60}(Ce_{0.22}Y_{0.18})O_{1.61}$ only the C-type cubic ordered phase was present with the complete disappearance of the monoclinic phase. The cubic lattice parameters decrease steadily from the composition $Nd_{0.60}(Ce_{0.22}Y_{0.18})O_{1.61}$ to the composition $Nd_{0.05}(Ce_{0.52}Y_{0.43})O_{1.761}$ (or increase with increase in Nd^{3+} content) as shown in Fig. 4(c). This trend in lattice parameter is again due to the fact that more and more Y^{3+} are being substituted for Nd^{3+}.

The ternary phase relations in CeO_2–$YO_{1.5}$–$NdO_{1.5}$ system are summarized in Fig. 7. It would be important to comment here that the present work involves phase relations in the given system under very slow-cooled conditions. There are certain regions in the ternary phase relations (Fig.7) wherein existence of certain phase fields might not conform to the phase rule. To

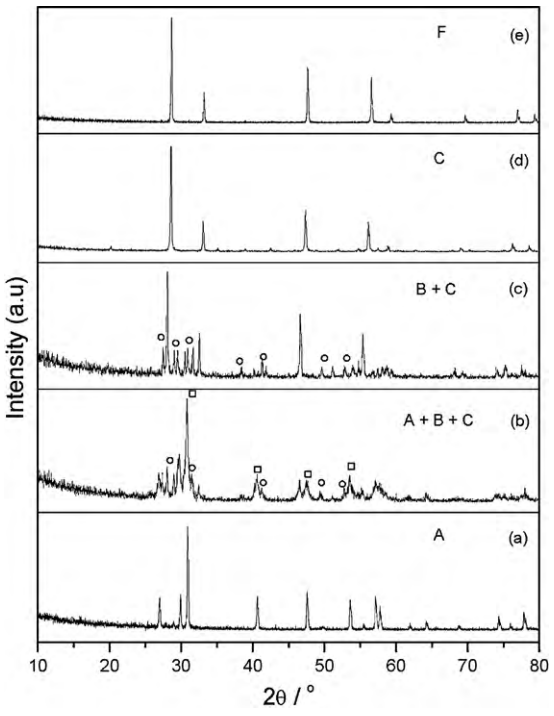

Fig. 6. XRD patterns in $Nd_{1-x}(Ce_{0.55}Y_{0.45})_xO_{1.5+0.275x}$ system: (a) Nd_2O_3; (b) $Nd_{0.95}(Ce_{0.028}Y_{0.022})\ O_{1.513}$; (c) $Nd_{0.80}(Ce_{0.11}Y_{0.09})\ O_{1.55}$; (d) $Nd_{0.40}(Ce_{0.33}Y_{0.27})\ O_{1.665}$; (e) $Ce_{0.55}Y_{0.45}O_{1.775}$.

quote a specific example, in Fig.7 near the top of the triangle, the left boundary is denoted as the phase region (C + A), the right boundary is B phase, hence in accordance with the phase rule, we should have observed a wide A + B + C in the middle. Very careful observation shows that one of the compositions in between, i.e., $Nd_{0.95}(Ce_{0.028}Y_{0.022})O_{1.513}$ does show A + B + C phase field. However, had it not been a slow-cooled study and if we had observed the phases at equilibrium, we could have observed a wider triphasic phase field here. Hence it would be more apt to describe this study as the phase relation study rather than an equilibrium phase diagram.

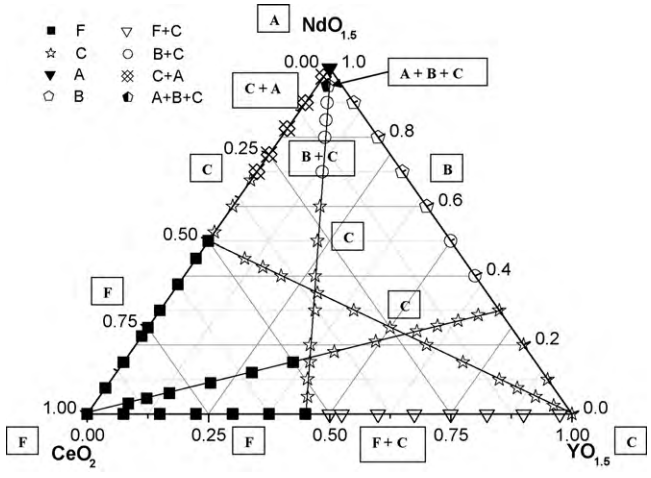

Fig. 7. Ternary phase relation in CeO_2–$YO_{1.5}$–$NdO_{1.5}$ system.

4. Conclusion

Detailed phase relation has been established in the CeO_2–$YO_{1.5}$–$NdO_{1.5}$ system for the first time. A wide range of solid solutions was observed throughout the system. All the ternary series show interesting phase developments. Thus whereas in the case of the $Ce_{1-x}(Y_{0.70}Nd_{0.30})_xO_{2-0.5x}$ series, there was a gradual transformation from the defective F-type cubic lattice to an ordered C-type phase (with increase in the x composition), $Y_{1-x}(Ce_{0.50}Nd_{0.50})_xO_{1.5+0.25x}$ series showed the existence of the C-type cubic lattice of $YO_{1.5}$ throughout the entire range. For the $Nd_{1-x}(Ce_{0.55}Y_{0.45})_xO_{1.5+0.275x}$ series, for the compositions with $NdO_{1.5}$ content up to 95 mol%, there was a coexistence of hexagonal phase along with a monoclinic and cubic phase. With decreasing content of $NdO_{1.5}$ from 90 to 70 mol% a biphasic region of monoclinic and C-type cubic phase was observed.

References

1. Kiork RE, Othmer DF. Cerium cerous compounds. In: *Encyclopedia of chemical technology, vol. 5*. 3rd ed. New York: Wiley; 1979, 315 pp.
2. Lee YW, Kim HS, Kim SH, Young CY, Na SH, Ledergerber G, et al. Preparation of Simulated inert matrix fuel with different powders by dry-milling method. *J Nucl Mater* 1999;**274**:7–14.
3. Ganguly C. ThO_2-based fuels for PHWRs: fabrication, characterization, and test irradiation. In: Hasting I, editor. *Proceedings of the IInd International Conference CANDU Fuel, Pembroke, Ontario, Canada*. 1989, 398 pp.
4. Strekalvskii VN, Burov GV, Samarina VA, Palguev SF, Volchenova ZS. Tr. Inst. Elektrokhim., Akad Nauk SSSR, Ural, Filial 1962;**3**:171.
5. Keler EK, Godina NA, Kalinina AM. The reaction of cerium dioxide with the oxides of the alkaline-earth metals. *Russ J Inorg Chem* 1956;**1**:127.
6. Moebius HH, Witzmann H, Zimmer F. Rontgenographische Untersuchungen an Fluoritphasen in den Systemen des Scandiumoxides mit Zirkon-Ceram. -und Thoriumdioxid. *Z Chem* 1964;**4**:194.
7. Bevan DGM, Barker WW, Martin RL. Mixed oxides of the type [2MO] (fluorite)–M_2O_3. Part 2. In non-stoichiometry in ternary rare-earth oxide systems. In: *Proceedings of the 4th Conference on Rare-Earths Research, Phoenix, AZ*. 1964.
8. Bruno M, Mayer A. Indagini sui Disordini Reticolari del Reticolo Fiuoriticoe del Reticolo Cubico Degli. *Ric Sci* 1958;**28**:1168.
9. Li L, Van Der Biest O, Wang PL, Leugels JV, Chen WW, Huang SG. Estimation of the phase diagram for the ZrO_2–Y_2O_3–CeO_2 system. *J Eur Ceram Soc* 2001;**21**:2903–10.
10. Hinatsu Y, Muromura T. Phase relations in the systems ZrO_2–Y_2O_3–Nd_2O_3 and ZrO_2–Y_2O_3–CeO_2. *Mater Res Bull* 1986;**21**:1343–9.
11. Benan A, Hrovat M, Holc J, Kosec M. Subsolidus phase equilibria in the RuO_2–Y_2O_3–CeO_2 system. *Mater Res Bull* 2000;**35**:2415–21.
12. Huang K, Feng M, Goodenough JB. Bi_2O_3–Y_2O_3–CeO_2 solid solution oxide-ion electrolyte. *Solid State Ionics* 1996;**89**:17–24.
13. Du Y, Yashima M, Koura T, Kakihana M, Yoshimura M. Measurement and calculation of the ZrO_2–CeO_2–$LaO_{1.5}$ phase diagram. *CALPHAD* 1996;**20**:95–108.
14. Grover V, Tyagi AK. Phase relation studies in CeO_2–Gd_2O_3–ZrO_2 system. *J Solid State Chem* 2004;**177**:4197–204.
15. Grover V, Tyagi AK. Sub-solidus phase equilibria in the CeO_2–ThO_2–ZrO_2 system. *J Nucl Mater* 2002;**305**:83–9.
16. Kleykamp H. The chemical state of the fission products in oxide fuels. *J Nucl Mater* 1985;**131**:221–46.
17. Sibieude F, Foex M. Phases et transitions de phases a haute temperature observers dan les systemes ThO_2–Ln_2O_3 (Ln = lanthanide et yttrium). *J Nucl Mater* 1975;**56**:229–38.

18. Keller C, Berndt U, Engerer H, Leitner L. Phasengleichgewichte in den systemen Thoriumoxid-Lanthanidenoxide. *J Solid State Chem* 1972;**4**:453–65.
19. Brauer G, Gradinger H. Über heterotype Mischphasen bei Seltenerdoxyden. *I Z Anorg Allg Chem* 1954;**276**:209–26.
20. Mccullough JD, Britton JD. X-ray studies of rare earth oxide systems. II. The oxide systems Ce^{IV}–Sm^{III}, Ce^{IV}–Gd^{III}, Ce^{IV}–Y^{III}, Pr^{IV}–Y^{III} and $Pr^{III}Y^{III}$. *J Am Chem Soc* 1952;**74**:5225–7.
21. Bevan DJM, Barker WW, Martin RL, Parks TC. In: Eyring L, editor. *Rare earth research, vol. 3*. New York: Gordon & Breach; 1965, 441 pp.
22. Hyde BG, Eyring L. In: Eyring L, editor. *Rare earth research, vol. 3*. New York: Gordon & Breach; 1965, 623 pp.
23. Pepin JG, Vance ER, Mccarthy GJ. Subsolidus phase relations in the systems CeO_2–RE_2O_3 (RE_2O_3 = C-type rare earth sesquioxide. *J Solid State Chem* 1981;**38**:360–7.
24. Chavan SV, Mathews MD, Tyagi AK. Phase relation and thermal expansion studies in ceria–yttria system. *J Am Ceram Soc* 2004;**87**:1977–80.
25. Chavan SV, Mathews MD, Tyagi AK. Phase relations and thermal expansion studies in the ceria–neodymia system. *Mater Res Bull* 2005;**40**:1558–68.
26. Grover V, Tyagi AK. Phase relations, lattice thermal expansion in CeO_2–Gd_2O_3 system, and stabilization of cubic gadolinia. *Mater Res Bull* 2004;**39**:859–66.
27. Banerji A, Grover V, Sathe V, Deb SK, Tyagi AK. CeO_2–Gd_2O_3 system: unravelling of microscopic features by Raman spectroscopy. *Solid State Commun* 2009;**149**:1689–92.
28. Adachi G, Imanaka N. The binary rare earth oxides. *Chem Rev* 1998;**98**:1479–514.